JOURNAL OF AGRICULTURAL AND FOOD CHEMISTRY

ARTICLE

pubs.acs.org/JAFC

Synthesis of Soybean Oil-Based Polymeric Surfactants in Supercritical Carbon Dioxide and Investigation of Their Surface Properties

Zengshe Liu* and Girma Biresaw

Bio-Oils Research Unit, National Center for Agricultural Utilization Research, Agricultural Research Service, U.S. Department of Agriculture, 1815 North University Street, Peoria, Illinois 61604, United States

ABSTRACT: This paper reports the preparation of polymeric surfactants (HPSO) via a two-step synthetic procedure: polymerization of soybean oil (PSO) in supercritical carbon dioxide followed by hydrolysis of PSO (HPSO) with a base. HPSO was characterized and identified by using a combination of FTIR, ^{1}H NMR, ^{13}C NMR, and GPC methods. The effects of HPSO polysoaps on the surface tension of water and interfacial tension of water−hexadecane were investigated as a function of concentration of HPSO and counterion chemistry. HPSO polysoaps were effective at lowering the surface tension of water and the interfacial tension of water−hexadecane. They displayed minimum values of surface tension in the range of 20.5−39.6 dyn/cm at a concentration range of 3.2−32 μM and minimum values of interfacial tension in the range of 15.6−31.44 dyn/cm. The minimum surface and interfacial tension values were highly dependent on the nature of the counterion and increased in the order $K^+ < Na^+ < TEA^+$. These results suggested that a very low concentration of surfactant can be used to reduce the surface tension of water and interfacial tension of water−hexadecane. Water−hexadecane interfacial energy was also calculated from measured surface tension data using Antonoff, harmonic mean (HM), and geometric mean (GM) methods. Measured values agreed well with those calculated using the HM and GM. The HM method predicted slightly higher values than the GM method, but the Antonoff method did not agree with measured values.

KEYWORDS: polymeric surfactants, soybean oil, supercritical carbon dioxide, surface tension, interfacial tension

INTRODUCTION

In recent years, increases in the emission of greenhouse gases, carbon dioxide and carbon monoxide, caused by the use of fossil fuels, such as petroleum and coal, have potentially resulted in a rapid advance in climate change. Hence, there is an urgent call for the reduction of carbon dioxide emissions. This condition has raised interest in the use of biodegradable polymers from inexpensive renewable resources to replace conventional polymers made from petroleum, a limited natural resource. Furthermore, the utilization of renewable raw materials can, in some cases, meet other principles of green chemistry such as biodegradation and lower toxicity of the resulting products.[1]

Among synthesized biobased products from agricultural resources, such as plant oils, polysaccharides (mainly cellulose and starch), sugars, wood, and others, plant oils are the most important raw material in the synthesis of fine chemicals, monomers and polymers. Approximately 80% of the global oil and fat production is vegetable oil, whereas 20% is of animal origin, the share of which has been decreasing recently.[2] Among vegetable oils, about 20% is soybean oil (SO), followed by palm, rapeseed, and sunflower oils. In the United States, soybean is the second largest farm crop, trailing only corn in annual planted acreage. In 2006, 86.9 million tons of soybean was grown in the United States, far in excess of the current market demand for U.S. soybean.[3] Annually, the United States produces about 1 billion pounds of SO in excess of current commercial demand. Therefore, there is a need to develop new uses for surplus soybean to prevent price depression due to oversupply.

SO is a triglyceride consisting of 11% palmic, 4% stearic, 23% oleic, and 8% linolenic acids. SO contains approximately 4.5 carbon−carbon double bonds per triglyceride. These double bonds are reactive sites and allow for the development of SO for various applications including inks, paints, biodiesel, lubricants, and cosmetic products.[4−8] The applications of triglycerides in the areas of coatings and resins were reviewed by Güner and coworkers[9,10] with a focus on cross-link systems for coating and resin applications. They concluded that triglycerides are expected to play a key role in the 21st century in the synthesis of polymers from renewable sources.[9,10]

In the past few years, attention has been focused on the development of environmentally friendly replacements for volatile organic solvents used for chemical reactions and materials processing.[11−15] One promising replacement candidate is supercritical carbon dioxide ($scCO_2$). The low toxicity of CO_2 and lack of toxic solvent residues in the final products make CO_2 an attractive medium for the synthesis and processing of polymers and biomaterials.[16−18] CO_2 is also inexpensive, readily available, and nonflammable. Products using natural oils as raw materials through $scCO_2$ or liquid CO_2 reaction or process media have been labeled "green materials". Although it is challenging to use pressure vessels for polymerization because of safety and cost efficiency issues, by using this green process, the high molecular weights of polymers are prepared with faster reaction rate, compared to the heat polymerization of vegetable oils with high temperature at 300 °C, long reaction time, and lower molecular weights of polymers obtained.

In a previous study, we investigated the modification of the carbon−carbon double bond in SO into epoxy groups (epoxidized soybean oil, ESO) and prepared polymeric soaps (HPESO) via a

Received: September 15, 2010
Accepted: January 11, 2011
Revised: January 11, 2011
Published: February 11, 2011

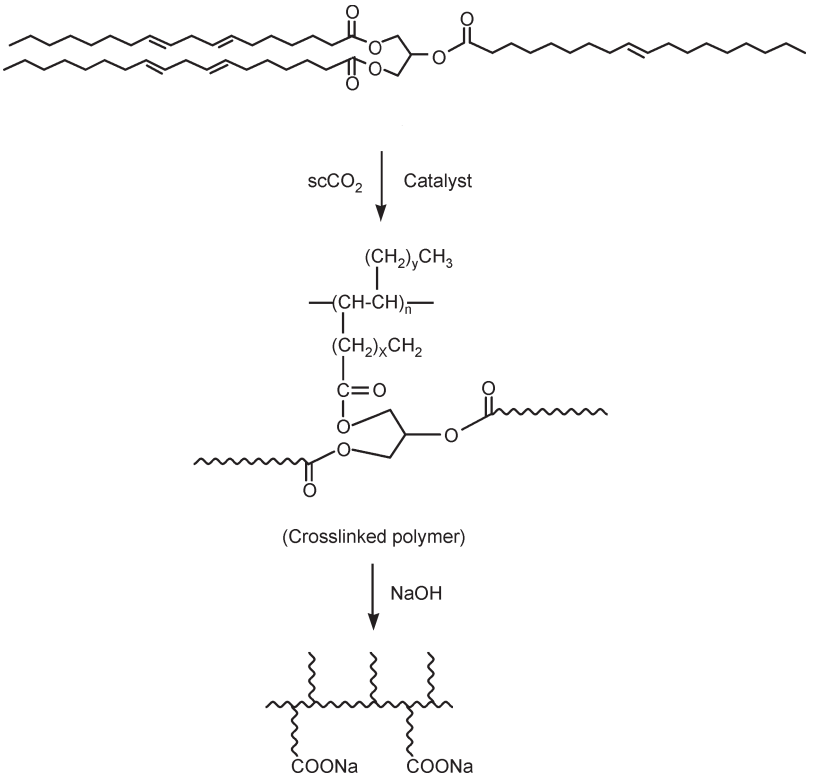

Figure 1. Reaction scheme used in the synthesis of HPSO polysoaps from soybean oil.

two-step synthetic procedure of catalytic ring-opening polymerization of ESO, followed by hydrolysis of PESO with a base.[19] The counterion was varied by changing the base used for saponification. HPESO polysoaps were effective at lowering the surface tension of water and the interfacial tension of water−hexadecane and displayed minimum values in the range of 20−24 and 12−17 dyn/cm, respectively, at concentrations of 200−250 μM. These HPESO polysoaps have a polyether (carbon−oxygen) backbone in the polymer chain. In this work, we report the direct conversion of SO into polymerized soybean oil (PSO) in $scCO_2$. Unlike HPESO, the polymer backbone of PSO is a carbon−carbon bond. The PSO was then converted into ionic polymeric surfactants (HPSO) by hydrolysis of PSO with a base (Figure 1). The surface-active properties of these polymeric surfactants (HPSO) were investigated. In addition, further studies were conducted comparing the surface properties of soy-based polysoaps with a carbon−carbon polymer backbone to the soy-based polysoaps with a carbon−oxygen polymer backbone.

EXPERIMENTAL PROCEDURES

Materials. Soybean oil (SO) was purchased from Purdue Farms Inc., Refined Oil Division (Salisbury, MD). Purified and redistilled boron trifluoride diethyl etherate, $(C_2H_5)_2O\cdot BF_3$, and triethanolamine (98%) were obtained from Sigma-Aldrich Co. (St. Louis, MO). Sodium hydroxide (97.5%) was obtained from Fisher Scientific (Fair Lawn, NJ), and potassium hydroxide (ACS agent, 88.3%) was obtained from J. T. Baker (Phillipsburg, NJ). Deionized water was purified to a conductivity of 18.3 MΩ-cm on a Barnstead model D8611 EASYpure UV/UF water purification system (Barnstead International, Dubuque, IA). Freshly purified water was then filtered on a 0.22 μL sterile disposable filter (MILLEX-GS 0.22 μL Filter Unit; Millipore Corp., Bedford, MA) prior to use in the preparation of aqueous (aq) polysoap solutions for surface and interfacial tension measurements. Hexadecane (99+% anhydrous) was obtained from Sigma-Aldrich Co. and was purified by filtering in a 5 cm diameter clean glass column (Kontes Glass Co., Vineland, NJ) filled with 35 g of silica gel (premium Rf grade, 20−45 μM, Sorbent Technology, Atlanta, GA) on top of 35 g of alumina (neutral standard activity I, 50−200 μM, Sorbent Technology). The filtered hexadecane gave an interfacial tension of 51.5 dyn/cm with purified water.

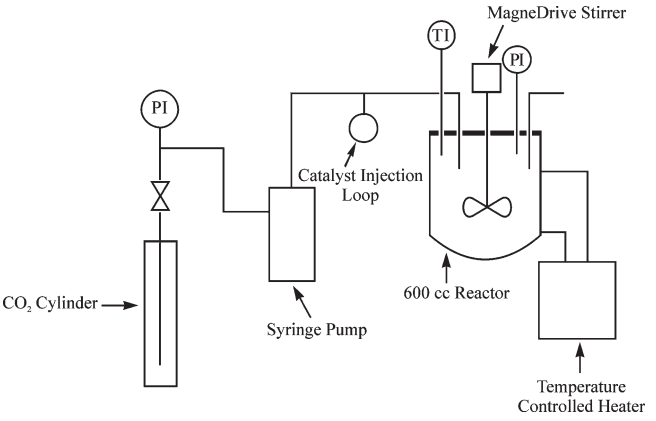

Figure 2. Schematics of reactor setup for the polymerization of soybean oil in $scCO_2$.

Polymerization of Soybean Oil in $scCO_2$. Polymerization reactions were carried out in a 600 mL pressure reactor from Parr Instrument Co. (Moline, IL). The schematic diagram of the experimental setup used for polymerization of SO is depicted in Figure 2. The reactor was attached to an Isco model 260D high-pressure syringe pump used to charge the reactor with CO_2. SO (100 g) was added to the reactor, which was then sealed. N_2 was purged into the reactor for 5 min. CO_2 was pumped in. A Parr model 4843 controller was used to control the temperature. Once the reactor brought the temperature to 100 °C, and pressure reached 1600 psi, $BF_3\cdot OEt_2$ (2.0 g) was charged into the

reactor by using a Rheodyne injector. Then CO_2 was pumped to clean the initiator supply line. After reaction for 24 h, 2 mL of ethanol/H_2O (1:1) solvent was added into the reactor to deactivate the catalyst. The resulting solid polymer product (PSO) was washed sequentially with H_2O, 5% aqueous sodium bicarbonate, and H_2O. The sample was then dried overnight under vacuum at 60 °C. Soxhlet extraction with hexane solvent was then used to remove the soluble substances. After 16 h of Soxhlet extraction, about 75 g of insoluble PSO product was obtained, which corresponded to 75 wt % yield.

Hydrolysis of Polymerized Soybean Oil (HPSO). Soybean-based polymeric soap (polysoap) was prepared by hydrolysis of PSO with alkaline base. A solution of 2.5 g of PSO in 50 mL of 0.4 N NaOH was refluxed for 24 h. The solution was then filtered with filter paper and cooled to room temperature. The resulting gel was precipitated with 1.0 N HCl (about 70 mL), followed by several washings with water and finally with two more washings with 10% (v/v) aqueous acetic acid. The resulting polymer was dried overnight at 80 °C in an oven. The sample was further dried under vacuum at 70 °C to a constant weight; 2.2 g (88% yield) of HPSO product was obtained.

Spectroscopic Identification of Synthetic Products. *Infrared (IR) Spectroscopy.* IR spectra were obtained on a Bomem MB-series Arid Zone FTIR spectrometer (Québec, Canada) equipped with a deuterated triglycine sulfate detector. Absorbance spectra were acquired at a spectral resolution of 4 cm^{-1} and were signal-averaged over 32 scans. Interferograms were Fourier-transformed using cosine apodization for optimal linear response. Spectra were baseline corrected and normalized to the methylene peak at 2927 cm^{-1}.

Nuclear Magnetic Resonance (NMR) Spectroscopy. ^1H and ^{13}C NMR spectra for SO and HPSO samples were recorded using a Bruker ARX-500 spectrometer (Rheinstetten, Germany) at observing frequencies of 500.13 (^1H) and 125.77 (^{13}C) MHz on a 5 mm dual probe. For ^1H and ^{13}C experiments, sample solutions were prepared in deuterated chloroform ($CDCl_3$, 99.8% D, Sigma-Aldrich) in 15 and 30% v/v concentrations, respectively. Proton NMR spectra were obtained after 16 scans at a delay time of 1 s. The integration values in the ^1H spectra were referenced to 4.00 ppm in the range of 4.1−4.44 ppm.

Determination of the Molecular Weight of HPSO. GPC profiles were obtained on a Polymer Laboratories (PL) model 120 GPC high-temperature chromatograph (Amherst, MA) equipped with a built-in differential refractive index detector and an autosampler. The flow rate was 1.00 mL/min at 40 °C. The injection volume was 100 μL. Linear polystyrene standards (PL, M_n = 580−100K, M_w/M_n = 1) were used for calibration of molecular weight of HPSO. Two PL gel 3 μm mixed E columns (300 mm × 7.5 mm) in series were used to resolve the samples. THF was used as the eluent.

Preparation of HPSO Polysoaps with Different Counter Ions. Stock solutions of 1.0 wt % aqueous HPSO−Na^+, K^+, and $(HOC_2H_5)_2N^+$ (TEA^+) were prepared according to the following procedure: 1.0 g of HPSO sample was weighed into a 50 mL beaker and the required amount of NaOH or KOH (to neutralize all of the acidic protons from carboxylic acid groups) was dissolved in 10 mL of water (18.3 mΩ). The beaker containing the HPSO sample and base solution was then placed in a 75 °C water bath and stirred with a glass rod until the HPSO sample dissolved. The resulting solution was then transferred to a 100 mL volumetric flask. The beaker was rinsed three times with 10 mL of water and added to the volumetric flask. The solution was then cooled to room temperature and filled with water to the 100 mL mark. The aqueous stock solution of HPSO−TEA salt was prepared by using a 2.5:1 molar ratio of triethanolamine (TEA) to carboxylic acid group in HPSO.

Dynamic Surface and Interfacial Tension. Dynamic surface and interfacial tension measurements were conducted using the axisymmetric drop shape analysis (ADSA) method[20] on a First Ten Angstroms (FTA) model 200 automated goniometer (Portsmouth, VA) equipped with FTA32 v2.0 software. In ADSA, interfacial tension was obtained by analyzing the change in the shape of a pendant drop of one liquid suspended in air or in a second liquid. The method is based on the Bashforth−Adams equation, which relates drop shape to interfacial tension.[21,22] A detailed description of the main features of the FTA 200 has been given previously.[19] All dynamic surface and interfacial tension measurements were conducted at room temperature (23 ± 2 °C) using the procedure described previously.[19] At the end of each measurement, the instrument displays and saves a plot and a spreadsheet of time versus surface or interfacial tension. Each concentration of aqueous HPSO solution was used in four to six repeat measurements, from which equilibrium surface or interfacial tension values were obtained by averaging the values at very long periods, over which the surface or interfacial tension values showed little or no change with time. Prior to running tests with the polysoap solutions, the instrument was calibrated with water and then checked by measuring the interfacial tension between water and purified hexadecane.

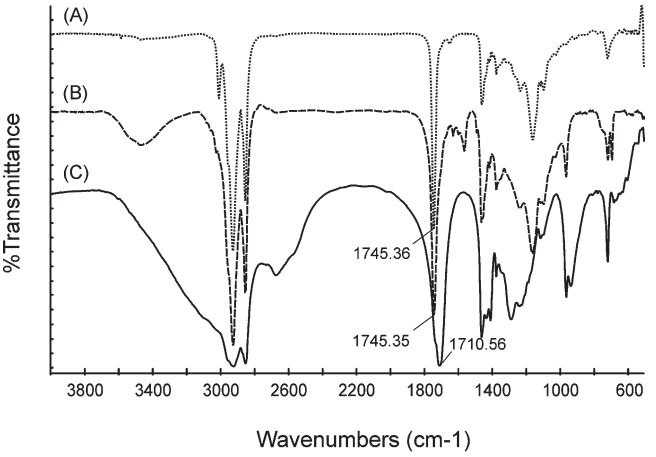

Figure 3. FTIR spectra of ESO (A), PSO (B), and HPSO (C).

Data Processing. Data from repeat measurements of surface and interfacial tension were used to calculate average and standard deviations for each sample. These values were plotted and/or analyzed further using IgorPro version 5.0.3.0 software (WaveMetrics, Inc., Lake Oswego, OR).

RESULTS AND DISCUSSION

Spectroscopic Identification of the Structures of HPSO Surfactants. *FTIR.* The infrared spectra of SO (A), PSO (B), and HPSO (C) are shown in Figure 3. The characteristic ester carbonyl absorption at 1745 cm^{-1} in ESO and PSO is clearly observed. The IR spectrum of the HPSO (Figure 3C) is for a sample obtained by hydrolysis of PSO with NaOH. The spectra of HPSO shows a shift in the ester carbonyl band from 1745 to 1710 cm^{-1} relative to PSO. This is attributed to strong H-bonding between carboxylic acids forming dimers. Hydrogen bonding weakens the C═O bond, resulting in an absorption shift to a lower frequency.

^1H NMR. Figure 4A shows ^1H NMR spectra of SO and HPSO. The signals at 5.40 ppm were characteristic for olefinic hydrogens, and those at 5.1−5.3 ppm represented the methine proton ($-CH_2-C\mathbf{H}-CH_2-$) of the glycerin backbone. The signals at 4.0−4.4 ppm were from the methylene protons ($-C\mathbf{H}_2-CH-C\mathbf{H}_2-$) of the glycerin backbone. The peak at 2.80 ppm corresponded to the bis-allylic $C\mathbf{H}_2$ protons, that is, the protons between two carbon−carbon double bonds. The signals at 2.10 ppm were allylic $C\mathbf{H}_2$ protons, that is, protons adjacent to carbon−carbon double bonds. As seen in Figure 4A, the peaks at 5.1−5.4 and 2.10 ppm in the ^1H NMR spectra of HPSO are greatly diminished

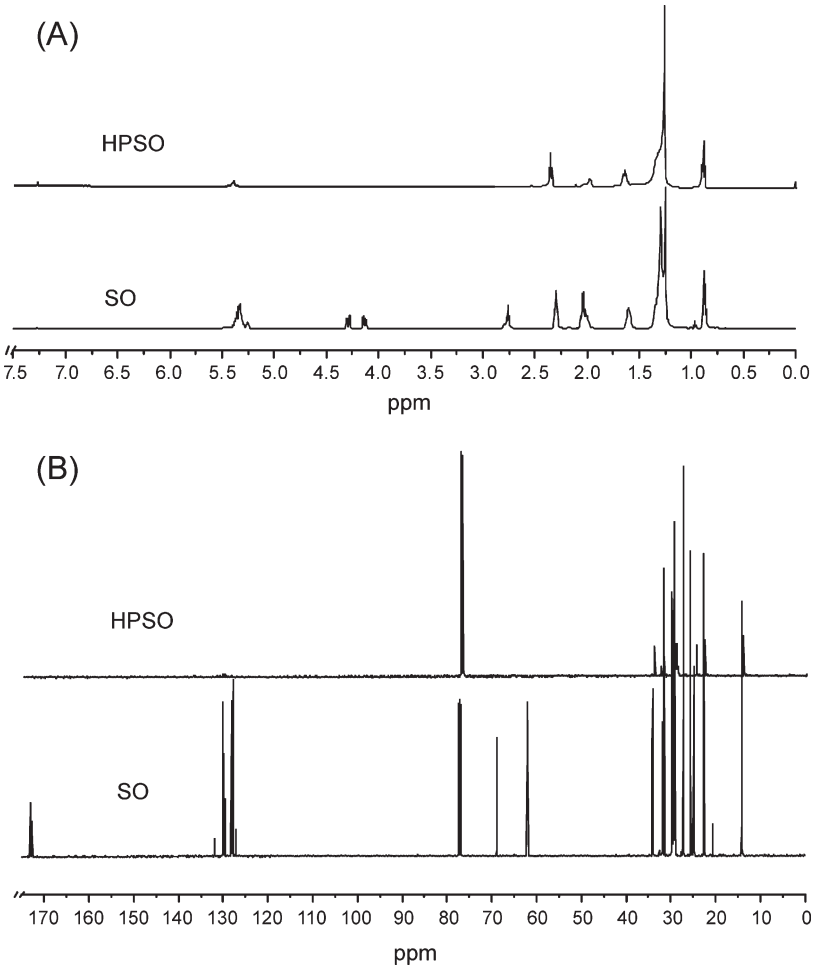

Figure 4. ^{1}H NMR (A) and ^{13}C NMR (B) of SO and HPSO.

compared to those of SO. The peak at 2.80 ppm completely disappeared in the ^{1}H NMR spectrum of HPSO. These observations indicated that polymerization of SO had occurred, and the number of carbon−carbon double bonds was greatly reduced.

^{13}C NMR. Figure 4B shows the ^{13}C NMR spectra of SO and HPSO. The ^{13}C NMR spectra confirmed that the polymerization of SO has occurred. For example, the peaks at 127−132 ppm in the ^{13}C NMR spectrum of SO were due to olefinic carbons and disappeared in the spectrum of HPSO. In addition, the signal at 173 ppm in the spectrum of SO assigned to the ester carbonyl carbon also disappeared in the spectrum of HPSO. This was because the hydrolysis converted the ester carbonyl carbon into a carboxylate salt.

GPC Determination of the Molecular Weight of HPSO. The molecular weight value of HPSO was determined by GPC. The GPC profile is shown in Figure 5, and results indicated that a molecular weight of 6.3 kg/mol was achieved. This polymer was used to prepare HPSO polysoaps.

Surface Tension of Aqueous HPSO Polysoaps. A series of aqueous solutions of the HPSO polysoaps with Na^{+}, K^{+}, and TEA^{+} counterions were prepared and their dynamic surface tensions investigated. Table 1 shows a list of the concentrations investigated for each polysoap. Each solution was used in four to six dynamic surface tension measurements. A typical repeat measurement is shown in Figure 6. As can be seen in Figure 6, the dynamic surface tension measurements displayed excellent repeatability.

The data in Figure 6 are for 48 μM aqueous Na^{+} HPSO solution and display the familiar surface tension versus time profile. This profile has four main characteristics: a high initial surface tension; an initial sharp decrease of surface tension with time; a slow decline in surface tension during intermediate periods; and a constant surface tension at long periods of time. This profile is consistent with the generally accepted mechanism of amphiphile diffusion from the droplet bulk to the droplet−air interface. Initially, the concentration of polysoap at the interface is low and, as a result, the surface tension is high. This causes rapid diffusion of polysoap molecules to the interface, causing a rapid increase in surface concentration and a corresponding rapid decrease of surface tension. As the concentration of the polysoap molecules at the air−water interface approaches the equilibrium value, the diffusion slows, and so the rate of surface tension declines. At very long times, the concentration of polysoap at the interface reaches the equilibrium value and the surface tension becomes constant and independent of time. Such a profile was observed for all concentrations of HPSO polysoaps with all three counterions.

From the time versus surface tension data shown in Figure 6, the surface tension values that display little or no change with time were used to calculate the average and standard deviation equilibrium surface tension for each concentration of polysoap. This value corresponded to the static surface tension of the solution used in the dynamic surface tension measurement.

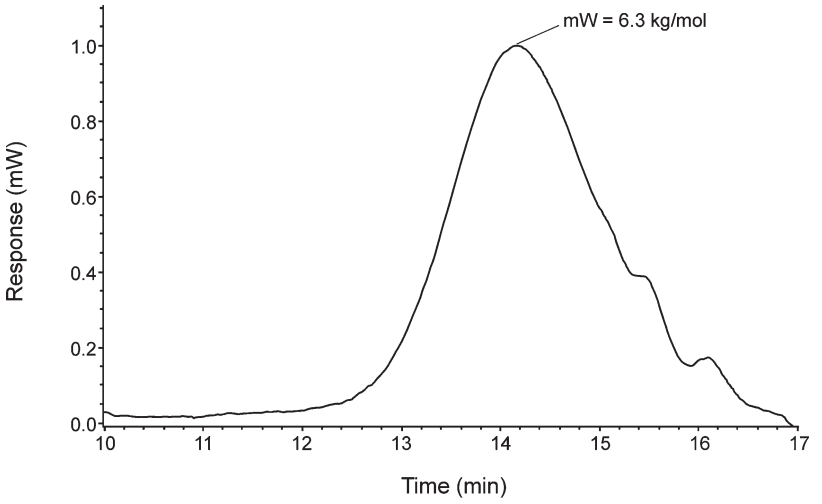

Figure 5. GPC trace of HPSO.

Table 1. Concentrations of Aqueous HPSO Polysoap Solutions Investigated

[Na^+ HPSO], μM	[K^+ HPSO], μM	[TEA^+ HPSO], μM
0	0	0
1.59	0.79	1.59
3.17	1.59	3.17
6.35	3.17	6.35
9.52	6.35	9.52
12.70	9.52	12.70
15.87	12.70	15.87
31.75	15.87	
47.62		

The equilibrium surface tensions for each of the solutions shown in Table 1 were calculated from the corresponding repeat measurements of dynamic surface tensions. The equilibrium surface tensions were highly dependent on the concentration of the polysoap. The higher the concentration of the polysoap in water, the higher its equilibrium surface concentration and the lower its equilibrium surface tension. This trend continues until the equilibrium surface concentration reaches full surface coverage and the surface tension reaches its minimum value. Further increase of polysoap concentration in water beyond this point will not result in an increase in surface concentration or a further decrease of surface tension.

The above-discussed phenomenon is illustrated in Figure 7, in which the equilibrium surface tensions of the three HPSO polysoaps are plotted as a function of concentration. As shown in Figure 7, the equilibrium surface tension of each polysoap decreased with increasing concentration and then leveled off to an essentially constant minimum value at very high concentrations. The concentration at which the equilibrium surface tension of the polysoaps stopped decreasing with concentration and began to become constant is referred to as the critical micelle concentration (CMC).[21,22] CMC is a characteristic property of amphiphiles (soaps, polysoaps, surfactants, etc.) and can be determined using a variety of methods including surface tension.[21,22] At the CMC, amphiphilic molecules spontaneously aggregate and form organized structures such as micelles. The lower the CMC, the more effective the amphiphile is at lowering surface tension of liquids.

The data in Figure 7 were used to determine the CMC and minimum equilibrium surface tensions of the three polysoaps investigated. The minimum equilibrium surface tensions were obtained by averaging the equilibrium surface tension values that remained constant with increasing concentration. The results are compared in Table 2. The data in Figure 7 and Table 2 indicated that both CMC and minimum equilibrium surface tension were affected by the nature of the counterion of the HPSO polysoap.

Similar minimum equilibrium surface tensions (20.5−22.5 dyn/cm) were obtained by HPSO polysoaps with K^+ and Na^+ counterions. These were about half of the value for HPSO polysoaps with the TEA^+ counterion (39.6 dyn/cm). The higher minimum equilibrium surface tension of TEA^+ HPSO polysoap implied a more polar interface was obtained when fully covered by TEA^+ polysoap than with Na^+ or K^+ polysoaps. This might be caused by the presence of TEA molecules at the interface because excess TEA^+ (2.5 equiv) was used to solubilize TEA^+ HPSO in water.

Comparison of CMC values showed that K^+ provided the most effective polysoap among the three counterions. The CMC of K^+ HPSO polysoap was 1 order of magnitude less than that of the Na^+ polysoap, even though these two counterions displayed similar minimum equilibrium surface tensions. The effectiveness of K^+ counterion relative to Na^+ might have to do with the relative sizes of these two ions. Because K^+ is larger than Na^+, it can attain full surface coverage with fewer polysoap molecules than Na^+.

Effect of HPSO Polysoap on Water−Hexadecane Interfacial Tension. The dynamic interfacial tension between aqueous HPSO polysoap solutions and hexadecane was obtained from analysis of the shape change with time of a pendant drop of the aqueous solution suspended in a hexadecane medium contained in a glass cuvette. Each of the solutions shown in Table 1 was used in four to six repeat measurements. A typical data set from such repeat measurement is illustrated in Figure 8. The data in Figure 8 are for a 12.7 μM aqueous solution of K^+ HPSO and showed an excellent repeatability between measurements.

The time versus interfacial tension data shown in Figure 8 displayed a profile similar to that of the time versus surface tension data discussed earlier. The profile had the following characteristic features: high initial interfacial tension, rapid decline of interfacial tension during early periods, slow decline of interfacial tension during intermediate periods, and constant interfacial tension at long periods. The reason the observed profile was similar to that

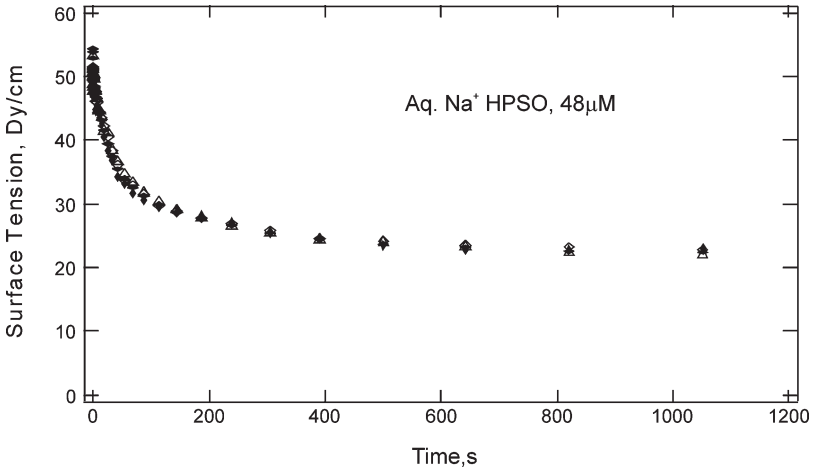

Figure 6. Repeat measurements of dynamic surface tension of water with 48 μM Na^+.

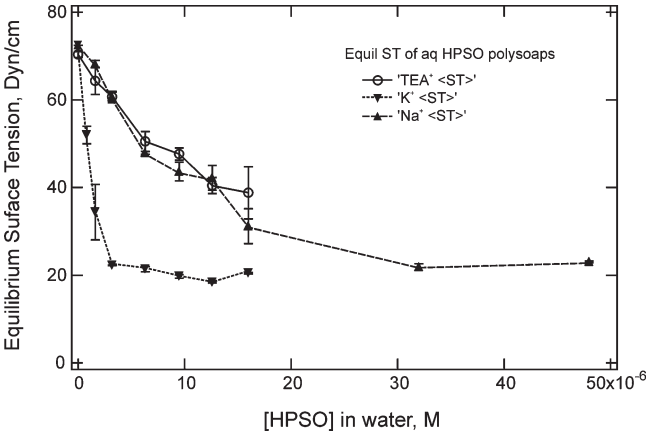

Figure 7. Effect of HPSO polysoap concentration in water on equilibrium surface tension of water.

Table 2. Average Minimum Equilibrium Surface Tension, $\langle ST_{min} \rangle$, and CMC of Aqueous HPSO Polysoaps

counterion	$\langle ST_{min} \rangle \pm$ SD, dyn/cm	CMC, μM
K^+	20.5 ± 1.5	3.17
Na^+	22.5 ± 0.8	31.7
TEA^+	39.6 ± 1.1	12.7

discussed earlier for dynamic surface tension is related to the diffusion of polysoap molecules from the aqueous phase to the water−hexadecane interface. Initially, the concentration of polysoap molecules at the interface is very low, and the interfacial tension will be very high, slightly below that of pure water−hexadecane, which is 51 ± 1 dyn/cm.[23] This will cause polysoap molecules to diffuse quickly from the water phase to the water−hexadecane interface, which will result in a rapid decline of interfacial tension early in the process. As time progresses, the concentration of polysoap molecules at the interface increases and approaches its equilibrium value. This will cause the rate of diffusion of polysoap molecules to the interface to slow, resulting in a slower decline of the interfacial tension. At very long times, the diffusion causes the concentration of polysoap molecules at the interface to attain its equilibrium value, which results in the equilibrium interfacial tension. Beyond this time, diffusion will not result in increased concentration of polysoap molecules at the interface, and the interfacial tension becomes constant and independent of measurement time (Figure 8).

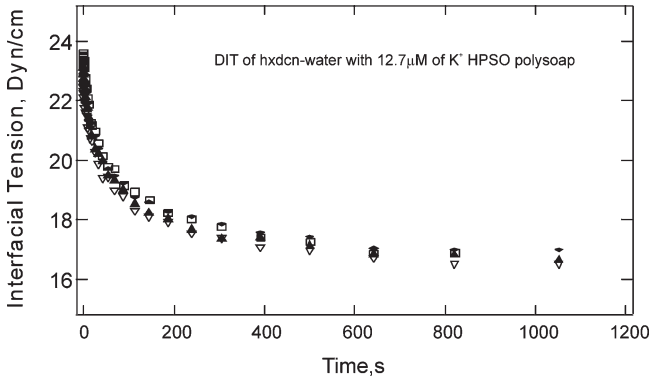

Figure 8. Repeat measurements of water−hexadecane dynamic interfacial tension in the presence of 12.7 μM K^+ HPSO polysoap.

The interfacial tensions at very long times correspond to the static or equilibrium interfacial tension for the interface under consideration. The equilibrium interfacial tension values were obtained by averaging the interfacial tension data points at very long times, which displayed little or no change with time. For example, for the hexadecane/aqueous K^+ HPSO system shown in Figure 8, the last three data points were used to calculate the average and standard deviation equilibrium interfacial tension value. Using similar procedures, the equilibrium interfacial tension values between hexadecane and the aqueous polysoap solutions listed in Table 1 were calculated from the corresponding dynamic interfacial tension data similar to that shown in Figure 8.

Equilibrium interfacial tension values were highly dependent on the concentration of the HPSO polysoap in the water phase. This was because the equilibrium concentration of polysoap molecules at the water−hexadecane interface was a function of the concentration of polysoap in the water phase. The higher the concentration of the polysoap in water, the higher its equilibrium concentration at the hexadecane−water interface and the lower the hexadecane−water interfacial tension obtained. This relationship between polysoap concentration in the water phase and the equilibrium hexadecane−water interfacial tension is illustrated in Figure 9. As shown in Figure 9, the equilibrium hexadecane−water interfacial

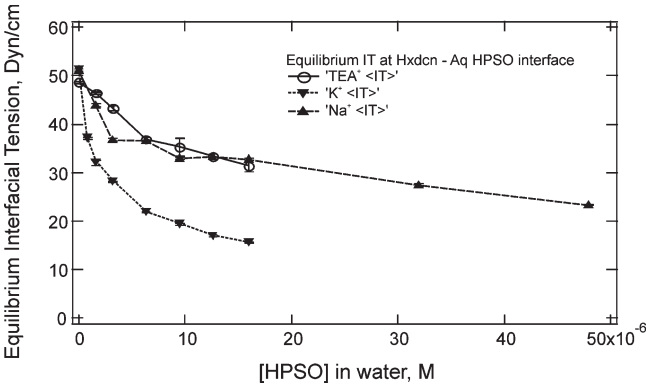

Figure 9. Effect of HPSO polysoap concentration in water on equilibrium water−hexadecane interfacial tension.

tension of polysoaps with all three counterions decreased with increasing concentration of polysoaps in water.

Examination of the data in Figure 9 indicated that the equilibrium interfacial tension values showed dependence on the nature of the polysoap counterion. Similar concentration−equilibrium interfacial tension profiles were obtained for TEA^+ and Na^+ polysoaps. On the other hand, K^+ polysoaps displayed a profile different from those of the other two counterions. The K^+ polysoaps were more effective at reducing the hexadecane−water equilibrium interfacial tension than TEA^+ and Na^+ polysoaps. The K^+ polysoaps were also more effective at lowering the surface tension of water, which explained their effectiveness at lowering the hexadecane−water equilibrium interfacial tension.

As the concentration of polysoap molecules in the water phase increased, the equilibrium hexadecane−water interfacial tension decreased until the concentration of polysoap molecules at the interface attained full coverage. At full interface coverage, the equilibrium interfacial tension attained its minimum value. Further increases of polysoap concentration in the water phase did not result in further increases in the concentration of polysoap molecules at the interface, and no further decrease of the equilibrium interfacial tension was observed. Thus, at concentrations of polysoaps in water beyond full interface coverage, the equilibrium interfacial tensions became constant and independent of polysoap concentration in water.

Examination of the data in Figure 9 showed that the equilibrium interfacial tension values for all three polysoaps decreased sharply at low concentrations. As the concentration of polysoap in water increased, the equilibrium interfacial tension decreased less severely. For the concentrations investigated in this work, it was clear that the equilibrium interfacial tension values for all three polysoaps were trending toward a constant value. This meant that the minimum hexadecane−water equilibrium interfacial tension values for each of the three polysoaps were slightly below the last data point shown in Figure 9. We consider these values, which are summarized in Table 3, as the minimum equilibrium interfacial tensions for the three polysoaps and use them in further analyses.

Surface and Interfacial Energy. The minimum equilibrium surface tension values given in Table 2 correspond to the surface energies of the corresponding polysoaps and can be used in further analyses. This is because the values were obtained on surfaces that were fully covered by the polysoaps. On the basis of similar considerations, the minimum equilibrium interfacial tensions given in Table 3 also correspond to the interfacial energies between polysoap molecules and hexadecane.

Table 3. Minimum Water−Hexadecane Equilibrium Interfacial Tension (IT) of HPSO Polysoaps

counterion	$IT_{min} \pm SD$, dyn/cm	[HPSO], μM
K^+	15.6 ± 0.1	15.9
Na^+	23.4 ± 0.1	47.6
TEA^+	31.4 ± 1.1	15.9

The surface energies of materials such as polysoaps, γ_S, comprise polar (γ_S^p) and dispersive (γ_S^d) components, which are related as follows:[24]

$$\gamma_S = \gamma_S^d + \gamma_S^p \quad (1)$$

The surface energies and their components can be used to estimate the interfacial energies of these materials with other surfaces using a variety of methods. The simplest of these methods is the Antonoff procedure,[25,26] which relies solely on the surface energies of the components and is expressed as

$$\gamma_{SH} = |\gamma_S - \gamma_H| \quad (2)$$

where γ_{SH} is the interfacial energy between the two surfaces (polysoap and hexadecane in this work) and γ^S, γ_H are the surface energies of the two surfaces.

Two other methods that utilize surface energies, along with the corresponding dispersive and polar components, are the harmonic mean (HM) and the geometric mean (GM), which give the following relationships, respectively:

$$\gamma_{SH} = \gamma_S + \gamma_H - \frac{4\gamma_S^d\gamma_H^d}{\gamma_S^d + \gamma_H^d} - \frac{4\gamma_S^p\gamma_H^p}{\gamma_S^p + \gamma_H^p} \quad (3)$$

$$\gamma_{SH} = \gamma_S + \gamma_H - 2(\gamma_H^d\gamma_S^d)^{0.5} - 2(\gamma_H^p\gamma_S^p)^{0.5} \quad (4)$$

In eqs 1−4 above, the subscripts S and H denote polysoap and hexadecane, respectively, whereas superscripts d and p denote dispersive and polar, respectively. Unlike the Antonoff method expressed in eq 1, application of the HM and GM methods requires knowledge of the polar and dispersive surface energy components of the materials. This is not a problem for one of the materials used here, hexadecane, which has a polar component of 0. Substitution of $\gamma_H^p = 0$ will eliminate the last terms in eqs 3- and 4 and result in significant simplification of the HM and GM methods. However, the simplified equations still require knowledge of the γ_S^d values to carry out the estimation of the interfacial energies. One way around this problem is to express the dispersive surface energy component of the polysoaps in terms of fractional nonpolar component, x_S^d as

$$\gamma_S^d = x_S^d\gamma_S \quad (5)$$

where $\chi_S^d = \gamma_S^d/\gamma_S$ and has values between 0 and 1.

Substitution of eq 5 and $\gamma_H^p = 0$ in eqs 3 and 4 yields the following simplified equations for the HM and GM methods, respectively:

$$\gamma_{SH} = \gamma_S + \gamma_H - \frac{4x_S^d\gamma_S\gamma_H}{x_S^d\gamma_S + \gamma_H} \quad (6)$$

$$\gamma_{SH} = \gamma_S + \gamma_H - 2(x_S^d\gamma_S\gamma_H)^{0.5} \quad (7)$$

Equations 2, 6, and 7 were used to estimate polysoap−hexadecane interfacial energies using the surface energies of the polysoaps given in Table 2. A value of 27.5 dyn/cm for the surface energy of hexadecane[22] and x_S^d as a fitting parameter with values

Table 4. Calculated versus Measured Interfacial Energy at the Polysoap−Hexadecane Interface

			polysoap−hexadecane IE, dyn/cm				
	MW, g/mol	SE ± SD	mean	X_S^d	calcd HM	calcd GM	calcd Ant
hexadecane	224	27.5					
K^+ HPSO	6300	20.5 ± 1.5	15.6 ± 0.1	0.4	22.7	18.0	7.0
Na^+ HPSO	6300	22.5 ± 0.8	23.4 ± 0.1	0.4	22.9	18.5	5.0
TEA^+ HPSO	6300	39.6 ± 1.1	31.4 ± 1.1	0.4	26.9	25.4	12.1
K^+ HPESO	2615	19.9 ± 0.6	11.9 ± 0.1	0.6	14.1	11.2	7.6
K^+ HPESO	3219	19.9 ± 1.1	12.7 ± 0.2	0.6	14.1	11.2	7.6
Na^+ HPESO	3219	21.6 ± 0.5	13 ± 0.04	0.6	13.9	11.3	5.9
TEA^+ HPESO	2615	22.9 ± 0.4	14.2 ± 0.1	0.6	13.8	11.5	4.6
TEA^+ HPESO	3219	23.9 ± 1.4	16.9 ± 0.2	0.6	13.7	11.7	3.3

between 0 and 1 were used. The estimated interfacial energies are summarized in Table 4 along with similar results for soy-based polysoaps with carbon−oxygen in the polymer backbone.[19] The two groups of polysoaps also differed from each other in their molecular weights. Despite these differences, the two sets of polysoaps displayed similar trends in the effect of counterions on surface and interfacial energies that decreased in the order $K^+ < Na^+ < TEA^+$ (Table 4). As shown in Table 4, the Antonoff method generally predicted much lower interfacial energy than was measured. This observation was true for both sets of polysoaps. The estimated interfacial energies of the HM and GM, however, depend on the selected value of x_S^d. Thus, for these two methods, the x_S^d value was varied to obtain estimated interfacial energy values as close to measured values as possible. For the HPSO polysoaps, a value of $x_S^d = 0.4$ gave estimated interfacial energy values close to measured values. The corresponding x_S^d value for the HPESO polysoaps was 0.6 (Table 4). The result showed that, for the same x_S^d value, the HM methods predicted slightly higher interfacial energy than the GM method.

The differences in the x_S^d values between HPSO and HPESO polysoaps were an indication of differences in surface properties between these polysoap materials. Lower x_S^d values corresponded to higher surface polarity. Thus, the data suggested that the HPSO polysoaps were more polar than the HPESO. This result was contrary to expectations based on the relative structures between these two materials, which are depicted in Figure 10. The HPESO polysoaps had a [−C−O−C−] linked repeat unit in their polymer backbone, whereas the HPSO polysoaps had only a [−C−C−] linked repeat unit. This difference should make the HPESO polysoaps more polar than the HPSO. The fact that the reverse was observed is an indication that a different mechanism was at work. We speculate the observed difference in the polarity between these materials had to do with the difference in their molecular weights. The molecular weight of HPSO molecules was at least twice those of HPESO. This meant that there were twice as many of the hydrophilic soap units per molecule in HPSO as in HPESO. Even though the number of the hydrophobic chain was also doubled in HPSO molecules, the net contributions of the hydrophilic and hydrophobic segments appeared to be different. It was clear from the x_S^d value of HPSO polysoap that the polar hydrophilic segments contributed more, resulting in a net polar polysoap.

AUTHOR INFORMATION

Corresponding Author

*Phone: (309) 681-6104. Fax: (309) 681-6524. E-mail: kevin.liu@ars.usda.gov.

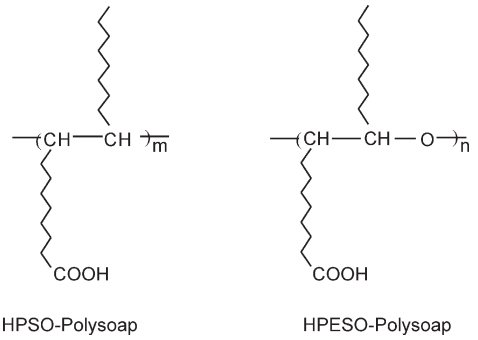

Figure 10. Comparison of repeat unit structures of HPSO versus HPESO polysoaps.

DISCLOSURE

Names are necessary to report factually on available data; however, the USDA neither guarantees nor warrants the standard of the product, and the use of the name by the USDA implies no approval of the product to the exclusion of others that may also be suitable.

ACKNOWLEDGMENT

We gratefully acknowledge Daniel Knetzer for help in GPC determination, Dr. Karl Vermillion for collecting NMR spectra, and Linda Cao for help with surface and interfacial tension measurements.

REFERENCES

(1) Eissen, M.; Metzger, J. O.; Schmidt, E.; Schneidewind, U. 10 years after Rio − concepts on the contribution of chemistry to a sustainable development. *Angew. Chem., Int. Ed.* **2002**, *41*, 414–436.

(2) Metzger, J. O.; Bornscheuer, U. Lipids as renewable resources: current state of chemical and biotechnological conversion and diversification. *Appl. Microbiol. Biotechnol.* **2006**, *71*, 13–22.

(3) Naeve, S. L.; Orf, J. H. *Quality of United States Soybean Crop*, 2006; available at http://www.unitedsoybean.org/library/rencnetLibraryIterms.aspx (2006 U.S. Soybean Crop Quality Survey, The United Soybean Board).

(4) Liu, K. *Soybeans Chemistry, Technology, Utilization*; Aspen Publishers: Gaithersburg, MD, 1999.

(5) Bockish, M. *Fats and Oils Handbook*; AOCS: Champaign, IL, 1998.

(6) The Soy Product Guide, United Soybean Board, 2006.

(7) *Industrial Uses of Vegetable Oils*; Erhan, S. Z., Ed.; AOCS Press: Champaign, IL, 2005.

(8) German Federal Ministry of Food, Agriculture and Consumer Protection, Agency of Renewable Resources; available at http://www.fnr.de.

(9) Güner, F. S.; Yagči, Y.; Erciyes, A. T. Polymers from triglyceride oils. *Prog. Polym. Sci.* **2006**, *31*, 633–670.

(10) Meier, M. A. R.; Metzger, J. O.; Schubert, U. S. Plant oil renewable resources as green alternatives in polymer science. *Chem. Soc. Rev.* **2007**, *36*, 1788–1802.

(11) Darr, J. A.; Polakoff, M. New directions in inorganic and metal-organic coordination chemistry in supercritical fluids. *Chem. Rev.* **1999**, *99*, 495–541.

(12) Beckman, E. J. Supercritical and near-critical CO_2 in green chemical synthesis and processing. *J. Supercrit. Fluids* **2004**, *28*, 121–191.

(13) Bektesevic, S.; Kleman, A. M.; Marteel-Parrish, A. E.; Abraham, M. A. Hydroformylation in supercritical carbon dioxide: catalysis and benign solvents. *J. Supercrit. Fluids* **2006**, *38*, 232–241.

(14) Dupont, J.; Consorti, C. S.; Spencer, J. Room temperature molten salts: neoteric "green"solvents for chemical reactions and processes. *J. Braz. Chem. Soc.* **2000**, *11*, 337–344.

(15) Liu, Z. S.; Doll, K. D.; Holser, R. A. Trifluoride catalyzed ring-opening polymerization of epoxidized soybean oil in liquid carbon dioxide. *Green Chem.* **2009**, *11*, 1774–1780.

(16) Butler, R.; Davies, C. M.; Cooper, A. I. Emulsion templating using high internal phase supercritical fluid emulsions. *Adv. Mater.* **2001**, *13*, 1459–1463.

(17) Cooper, A. I. Porous materials and supercritical fluids. *Adv. Mater.* **2003**, *15*, 1049–1059.

(18) Wood, C. D.; Tan, B.; Zhang, H.; Cooper, A. I. *Thermodynamics, Solubility and Environmental Issues*; Letcher, T., Ed.; Elsevier: Amsterdam, The Netherlands, 2007; Chapter 21, pp 383−396.

(19) Biresaw, G.; Liu, Z. S; Erhan, S. Z. Investigation of the surface properties of polymeric soaps obtained by ring-opening polymerization of epoxidized soybean oil. *J. Appl. Polym. Sci.* **2008**, *108*, 1976–1985.

(20) Rotenberg, Y.; Boruvka, L.; Neumann, A. W. Determination of surface tension and contact angle from the shapes of axisymmetric fluid interfaces. *J. Colloid Interface Sci.* **1983**, *93*, 169–183.

(21) Hiemenz, P. C. *Principles of Colloid and Surface Chemistry*, 2nd ed.; Dekker: New York, 1986.

(22) Adamson, A. P.; Gast, A. W. *Physical Chemistry of Surfaces*; Wiley: New York, 1997.

(23) Jasper, J. J. *J. Phys. Chem. Ref. Data* **1972**, *1*, 841.

(24) Wu, S. *Polymer Interface and Adhesion*; Dekker: New York, 1982.

(25) Antonoff, G. N. On the validity of Antonoff's rule. *J. Phys. Chem.* **1942**, *46*, 497–499.

(26) Antonow, G. N. Sur la tension superficielle des solutions dans la zone critique. *J. Chem. Phys.* **1907**, *5*, 364–371.